International Journal of Concrete Structures and Materials

RESEARCH Open Access

Performance-Based Durability Assessment of Low Carbon Concrete Using Electrical Resistivity

Jaehwan Kim[1], Ki-Tae Park[1] and Jinyoung Yoon[2*]

Abstract

A performance-based approach is essential for evaluating the long-term durability and performance of concrete. Nondestructive methods, such as electrical resistivity measurements, offer significant advantages in this context due to their simplicity, speed, and cost-effectiveness. This study applied electrical resistivity as a tool to assess key performance factors, including compressive strength and chloride transport properties, in concrete mixtures with and without supplementary cementitious materials (SCMs). The results demonstrated strong correlations between electrical resistivity and the performance factors across all concrete mixtures, highlighting its potential as a reliable evaluation method. While electrical resistivity shows promise for quantifying performance factors, challenges remain in addressing variability and measurement accuracy. Further investigations are recommended to refine the method and enhance its applicability in practical durability assessments.

Keywords Concrete performance, Durability, Electrical resistivity, Supplementary cementitious materials, Nondestructive testing

1 Introduction

The demand for reinforced concrete structures with a long service life is growing due to the need to offset increased initial costs and reduce environmental pollution. Achieving such longevity requires securing the durability of concrete throughout its service life. However, traditional prescriptive methods, which primarily focus on achieving a minimum compressive strength, are insufficient for evaluating or designing concrete with high durability. This is because compressive strength is only indirectly related to durability performance (ACI 318-19, 2019; Standard Specifications for Concrete Structures: Materials and Construction, 2007; Kessy et al., 2015). In other words, traditional concrete evaluation methods, i.e., prescriptive methods relying on 28-day compressive strength, fail to evaluate the long-term durability of sustainable concrete incorporating SCMs, such as fly ash (FA) and ground granulated blast-furnace slag (GGBS). These materials undergo prolonged hydration and pozzolanic reactions, refining the pore structures and enhancing chloride resistance over time. However, existing methods inadequately evaluate such characteristics. To address these limitations, performance-based approaches have gained attention as an alternative to prescriptive methods (Sangoju et al., 2021). Unlike prescriptive methods, performance-based approaches evaluate durability using parameters that are directly related to the deterioration mechanisms of concrete in aggressive environments, such as diffusion or migration coefficients, porosity, and electrical resistivity. As these parameters allow for a more accurate and reliable assessment of concrete durability, performance-based approaches are

*Correspondence:
Jinyoung Yoon
jyyoon@konkuk.ac.kr
[1] Department of Structural Engineering Research, Korea Institute of Civil Engineering and Building Technology, Goyang-Si, Gyeonggi-Do 10223, Republic of Korea
[2] Department of Civil and Environmental Engineering, Konkuk University, Seoul 05029, Republic of Korea

promising solutions for designing long-lasting structures, enabling optimized material selection and extended service life for low-carbon concrete.

Among the various deterioration processes that occur over time, chloride-induced corrosion is one of the most critical concerns for reinforced concrete structures. This form of corrosion is primarily caused by exposure to deicing salts or seawater (Yamamoto et al., 2024; Zhang et al., 2023). Chlorides penetrate the concrete, eventually reaching the steel reinforcement. Corrosion begins once the chloride concentration exceeds the tolerated threshold. Tuutti's model divides the service life of a reinforced concrete structure into two phases: (1) the corrosion initiation phase, during which chloride ions are transported and depassivation of the steel occurs, and (2) the corrosion propagation phase, characterized by the accumulation of corrosion products, cracking, and spalling of the concrete (Tuutti, 1982). While the propagation phase significantly impacts structural performance, the service life is typically defined by the end of the initiation phase, when depassivation occurs. This is because the propagation phase is relatively short and the quantification of corrosion rates in reinforced concrete is more challenging compared to the chloride transport mechanisms in the initiation phase. As specified, many studies on concrete durability have focused on understanding chloride transport processes, as these are critical for predicting the initiation phase and thus estimating the service life of structures (Sun et al., 2024; Tong et al., 2023).

To address the challenges associated with chloride transport and durability evaluation, durability indicators derived from laboratory tests have been extensively studied as key parameters for performance-based approaches (ASTM C1202-19, 2019; NT Build 492, 1999). These indicators, such as the migration coefficient obtained from chloride-accelerated tests, are essential for quantifying the transport properties and predicting the long-term durability of concrete. Effective durability assessment requires tests that are reliable, straightforward, and cost-effective. However, many traditional durability tests, such as compressive strength tests, chloride diffusion tests, and freeze–thaw tests, are destructive. This makes them impractical for continuous monitoring or repeated measurements over time. In addition, even when samples are fabricated from the same batch, discrepancies in test results can occur due to variability in sample preparation and testing conditions, resulting in scattered data. These limitations highlight the need for more reliable and efficient nondestructive testing methods.

It is well-known that concrete electrical flux tests (i.e., rapid chloride penetration test, RCPT) are generally used to determine the chloride transport property of concrete. Conventional methods apply DC voltage to concrete samples to penetrate the chloride solution into concrete rapidly, but there are some disadvantages as follows: (1) DC voltage can cause corrosion of steel in reinforced concretes; (2) the samples are no longer available due to contamination of chloride; and (3) the measurement time is relatively long (at least 6 h). On the other hand, electrical resistivity has emerged as one of the most attractive candidates for evaluating concrete performance and durability due to its ease of measurement and its link to concrete deterioration processes (Chidiac & Shafikhani, 2020; Tibbetts et al., 2020). Electrical resistivity is determined by the connected pores within the pore network filled with chemical solutions. Aggressive agents dissolved in the pore solution move through these connected pores, meaning that electrical resistivity is directly related to the resistance to chloride transport in concrete exposed to chloride environments. However, it is well-known that electrical resistivity is affected by several factors, including temperature (Kim et al., 2019), binder type (McCarter et al., 2005), moisture content (Alaswad et al., 2020), and experimental setup (Newlands et al., 2008). The use of supplementary cementitious materials (SCMs) further complicates the interpretation of resistivity values, as they alter the pore structure and chemistry (Cai et al., 2021; Huang et al., 2022). While previous studies have focused on qualitative methods—using resistivity ranges to classify concrete quality (McCarter et al., 2022)—applying a performance-based approach requires electrical resistivity to be treated as a quantified parameter. In this context, electrical resistivity must be related to established durability indicators, such as migration coefficients and compressive strength, to provide a reliable measure of concrete performance. To address the challenges in applying electrical resistivity as a durability indicator, a quantitative relationship between resistivity and key performance factors—such as migration coefficients and compressive strength—needs to be established. This relationship is essential for enhancing the applicability of electrical resistivity in performance-based approaches. However, limited studies have established quantitative relationships between electrical resistivity and key durability indicators, particularly in concrete incorporating SCMs.

This study addresses that gap by systematically measuring and analyzing the long-term resistivity, compressive strength, and chloride migration characteristics of SCM-based concretes. Our findings aim to enhance the performance-based durability assessment framework by providing reliable, non-destructive evaluation methods applicable to sustainable concrete materials. Specifically, the electrical resistivity responses of concrete, both with and without SCMs, were measured over a period of up to 365 days. These measurements were conducted prior

to determining the compressive strengths and migration coefficients. Based on the resistivity findings, quantitative relationships between electrical resistivity and the performance factors were identified, providing a robust framework for utilizing resistivity as a reliable indicator of concrete durability. Furthermore, performance approach using the electrical resistivity contributes to sustainability through lifecycle efficiency. By enabling repeated, non-destructive assessment, electrical resistivity testing reduces material waste and supports resource-efficient design decisions. Ultimately, this promotes the broader use of SCM-based concretes, reducing carbon emissions while ensuring structural performance.

2 Materials and Methods

2.1 Mixtures and Samples

To prepare testing samples, three binders were used: PC to KS L 5201 ("KS L 5201:2016 Portland cement" 2016), GGBS to KS L 5210 ("KS L 5210:2017 Portland blast-furnace slag cement" 2017), and FA to KS L 5405 ("KS L 5405:2018 Fly ash" 2018). GGBS and FA replaced PC at ratios of 40% and 30%, respectively. Based on these proportions, three mixture designs were developed with a water-to-binder ratio (w/b) of 0.4. The oxide compositions and mixture designs are presented in Tables 1 and 2. Crushed granite with a particle size of 4–20 mm was used as coarse aggregate, while fine aggregate with a particle size less than 4 mm was incorporated. Mixing was performed using a 0.1 m^3 capacity concrete pan mixer, ensuring uniformity within each batch. A water-reducing admixture conforming to KS F 2560 ("KS F 2560:2019 Chemical admixtures for concrete" 2019) was added to improve the workability of the mixtures.

Two types of samples were prepared for each mixture: (1) cylinders (Ø 100 × 300 mm) for migration tests and electrical resistivity measurements and (2) cubes (100 × 100 × 100 mm) for compressive strength and resistivity tests. Each type of sample was tested in triplicate. After casting, all samples were wrapped in polyethylene to prevent water evaporation from the concrete surface. After 24 h casting, the cube samples were demolded and cured in a water bath maintained at 20 ± 1 °C until testing. In contrast, the cylinders designated for the migration test were left in the molds during curing to minimize hydrate leaching and better simulate the conditions of core samples in real structures. For the migration test, cylindrical specimens were sectioned from the central region using a water-cooled saw. Each cylinder was cut into three specimens with dimensions of Ø 100 mm × 50 mm, and all tests were performed in triplicate.

2.2 Compressive Strength

Compressive strength tests were conducted in accordance with KS F 2405 ("KS F 2405:2010 Standard test method for compressive strength of concrete" 2010). For each mixture, three replicate samples were tested at curing ages of 28, 90, 180, and 365 days. Prior to the compressive strength tests, electrical resistance measurements were performed as described in Sect. 2.4. All samples were cured in a water bath maintained at 20 ± 1 °C, as described in previous section.

Table 1 Mixture design used in the sample

Mixture designation	PC (kg/m^3)	GGBS (kg/m^3)	FA (kg/m^3)	Aggregate (kg/m^3)	Sand (kg/m^3)	WR (l/m^3)	Slump (mm)
PC	460	–	–	1012	700	1.84	140
40GGBS	270	180	–	1016	745	1.35	100
30FA	370	–	160	890	635	1.59	130

PC Portland cement, *GGBS* ground granulated blast furnace slag, *FA* fly ash, *WR* water reducer

Table 2 Oxide compositions for binder types

Percentage composition by weight	SiO_2	Al_2O_3	Fe_2O_3	CaO	MgO	TiO_2	P_2O_3	SO_3	K_2O	Na_2O
PC	20.68	4.83	3.17	63.95	2.53	–	–	2.80	0.54	0.08
GGBS	51.00	27.40	4.60	3.40	1.40	1.60	0.30	0.70	1.00	0.20
FA	33.27	13.38	0.56	41.21	8.49	0.90	–	0.62	0.50	0.33

2.3 Chloride Analysis in Concrete

The migration coefficient is a critical input for transport-related properties of concrete in predictive models assessing performance and durability in chloride environments, as it is directly linked to diffusivity. The diffusion coefficient is often determined using regression analysis methods based on the "erf" function and chloride profile data from laboratory or field samples (Tang et al., 2012). Similarly, the migration coefficient $\left(D_{nssm} = \frac{RT}{zFE} \bullet \frac{(x_d - \alpha\sqrt{x_d})}{t}\right)$, determined using the NT Build 492 method (NT Build 492, 1999), is widely employed in models such as Duracrete (Altmann et al., 2012), ClinConc (Tang 2008), and LIFE 365 (M.Ehlen, 2014) to predict chloride transport in concrete. It is also specified in European codes as a key parameter for performance-based evaluations. Building on these methodologies, this study determined the migration coefficients of concrete samples to assess their performance in chloride environments, following the performance-based testing approach outlined in NT Build 492 (NT Build 492, 1999).

Prior to testing, the samples underwent vacuum saturation as specified in the standard. After saturation, electrical measurements were performed using an end-to-end electrode configuration. These measurements were conducted at curing ages of 180, 270, and 365 days. The test procedures strictly adhered to the specifications outlined for determining the migration coefficient. Upon completion of the migration test, the migration coefficient was calculated based on the chloride penetration depth, which was measured using a colorimetric method (NT Build 492, 1999).

2.4 Electrical Resistance Measurements

In this study, electrical resistivity measurement was employed as a nondestructive method to evaluate the performance and durability of concrete, particularly its relationship with compressive strength, migration coefficients, and degree of saturation. This method is increasingly used and has shown a good performance in concrete research to assess durability-related properties, such as pore structure, moisture content, and ion transport (Polder, 2001). Its non-invasive nature makes it particularly valuable for performance-based evaluations. Electrical resistivity has been widely applied in previous studies; however, several challenges associated with this method have been noted. Factors such as concrete inhomogeneity, pore solution composition, geometrical effects, and temperature variations significantly influence the results, making interpretation complex (Kurumisawa & Nawa, 2016). Furthermore, discrepancies in experimental setups—such as contact media, electrode pressure, and measurement frequency—can result in resistance variations of up to threefold (Newlands et al., 2008). For instance, a literature review revealed that the frequency range used for determining bulk resistance varied widely, typically between 50 Hz and 1 kHz (McCarter et al., 2015). These issues highlight the importance of a well-controlled experimental setup to ensure accurate and reliable measurements.

To address these challenges, we designed our experimental setup to minimize variability and ensure consistency in measurements. Resistivity was measured using the end-to-end method, which involved two stainless-steel plates and an LCR meter (HP 4263B, Manufacturer, City, State, Country). The LCR meter operated at a fixed frequency of 1 kHz and an applied voltage of 350 mV, as recommended for achieving reliable bulk resistance measurements. To maintain proper contact between the electrodes and the concrete surfaces, wetted synthetic sponges saturated with a $Ca(OH)_2$ solution were placed between the plates and the sample (Newlands et al., 2008). In addition, a 2 kg mass was applied to the upper electrode to ensure uniform pressure and reduce contact resistance variability. This carefully controlled setup ensured reliable and reproducible electrical resistivity measurements, which were performed prior to migration and compressive strength tests. The configuration of the end-to-end method is illustrated in Fig. 1, and the results were subsequently correlated with other performance parameters to assess the durability characteristics of the concrete mixtures.

The measured electrical resistance was converted into electrical resistivity, which was independent of the geometry of the sample:

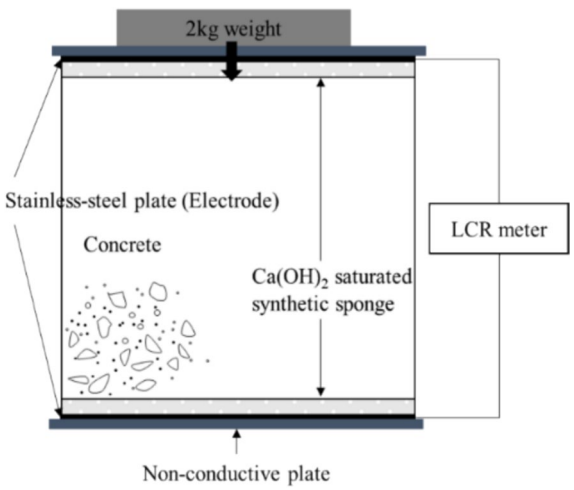

Fig. 1 Experimental setup used for electrical resistance measurements

$$\rho = \frac{R \bullet A}{L} \tag{1}$$

where ρ is the electrical resistivity (Ω·m), R is the electrical resistance (Ω), A is the cross-sectional area (m^2), and L is the thickness of the sample (m). Concrete is often characterized by its electrical resistivity, which serves as an indicator of its performance. While high electrical resistivity is generally associated with better durability and resistance to ionic transport, this measure is largely qualitative and requires additional context for comprehensive evaluation.

3 Experimental Results

3.1 Development of Compressive Strength

Although compressive strength is not a direct indicator of concrete durability (Alexander et al., 2008), it remains a critical reference parameter for quality control as specified in PD CEN 16563 ("PD CEN/TR 16563:2013 Principles of the equivalent durability procedure" 2013). Traditionally, compressive strength at 28 days is the benchmark; however, with the advancement of cementitious materials, performance evaluation often extends beyond this period to capture long-term durability and strength development. In this study, concrete exhibited rapid strength development during the first 28 days, followed by a more gradual increase thereafter. For mixtures incorporating pozzolanic or latent hydraulic binders, such as FA and GGBS, compressive strength developed more slowly but continued to increase over extended curing periods. This is attributed to the ongoing pozzolanic and hydration reactions associated with these materials. Figure 2 illustrates the average compressive strengths measured over a 365-day curing period, with markers representing test data and error bars indicating ± 1 standard deviation. The results show a clear trend of increasing compressive strength with curing ages. The observed development of compressive strength is modeled using best-fit curves derived from the BS EN 1992-1-1:2004 expression ("BS EN 1992-1-1:2004 + A1:2014 Eurocode 2: Design of concrete structures—Part 1–1: General rules and rules for buildings" 2014), emphasizing the correlation between curing duration and material strength:

$$f(t) = f_{\text{ref}} e^{s\left(1-(t_{\text{ref}}/t)^{0.5}\right)} \text{ MPa} \tag{2}$$

where $f(t)$ is the predicted compressive strength at age t (d), f_{ref} is the compressive strength at the reference age t_{ref} (=28 days), and the exponent s is a constant that indicates the rate of strength development. The best-fit curves for each mix are plotted with solid lines in Fig. 2 using the parameters listed in Table 3.

Compressive strengths of concrete samples containing SCMs were lower than those of PC concretes at an early age (less than 28-day curing). However, the strength increments from 28 to 365 days were significantly higher for GGBS concrete (46% for 40GGBS) and FA concrete (69% for 30FA) compared to PC concrete (44% for PC), primarily due to ongoing pozzolanic reactions (Hinrichs & Odler, 2015). The continuous strength increase in SCM concretes is attributed to the formation of an insoluble and dense calcium silicate hydrate (C–S–H) gel, which results from the reaction between siliceous oxides in SCMs and calcium hydroxide in the binder's pore solution. This process not only refines the pore structure but also enhances the chloride-binding capacity of the concrete (Yuan et al., 2009). As a result, the long-term development of compressive strength is a more reliable performance indicator for SCM concretes than the 28-day compressive strength.

This observation aligns with the s parameter values derived from best-fit models, where higher s values indicate slower strength development rates. The estimated s values were 0.46 for PC concrete, 0.50 for 40GGBS concrete, and 0.65 for 30FA concrete. These values confirm that concretes with SCMs exhibit slower, yet sustained, strength development over time. Regarding the performance-based evaluation, the use of time-dependent equations to estimate compressive strength is appropriate.

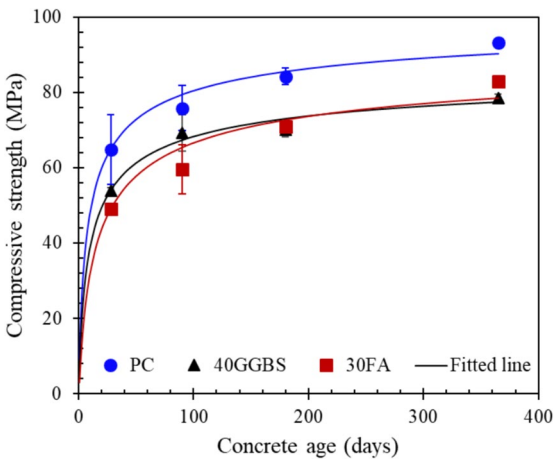

Fig. 2 Plots of compressive strengths as a function of concrete age

Table 3 Coefficients for best-fit curves derived from Eq. (2) in Fig. 2

Label	PC	40GGBS	30FA
f_{ref}(MPa)	64.88	53.93	50.00
s	0.46	0.50	0.65
R^2	0.95	0.96	0.91

3.2 Migration Coefficients

In this study, the migration coefficients of all mixtures were determined based on NT Build 492 method (NT Build 492, 1999):

$$D_{nssm\_measued} = \frac{0.0239 \times (273 + T) \times L}{(U - 2) \times t_{test}} \left[x_d - 0.0238 \sqrt{\frac{(273 + T) \times L \times x_d}{U - 2}} \right] (\times 10\ \mathrm{m2/s}) \quad (3)$$

where $D_{nssm\_measued}$ is the measured migration coefficient ($\times 10^{-12}$ m^2/s), U is absolute value of the applied voltage (V), T is average value of the initial and final temperature in the anolyte solution (°C), L is thickness of the specimen (mm), x_d is average value of the penetration depths (mm), and t_{test} is test duration (hour).

Figure 3 presents the migration coefficients of all mixtures over time. The markers represent mean values, and the error bars indicate ± 1 standard deviation. Concrete samples with SCMs exhibited significantly lower migration coefficients than PC concrete, with reductions ranging from 3.1 to 6.7 times. This enhanced resistance to chloride transport in SCM concretes is attributed to their finer pore structure and the continuous hydration reactions of SCMs (Huang et al., 2022). A general trend of decreasing migration coefficients with time was observed across all mixtures. The reductions in migration coefficients from 180 to 365 days were approximately 62% for GGBS concrete, 42% for FA concrete, and 30% for PC concrete.

These results highlight the durability advantages of SCM concretes in mitigating chloride transport. However, accurately capturing this phenomenon in computational models remains challenging. For instance, the ClinConc model uses migration coefficients at 180 days to estimate chloride profiles, assuming that the coefficient remains constant after this period, with reductions in chloride transport attributed primarily to chloride binding (Tang 2008). Applying this assumption to SCM concretes may result in overestimated chloride profiles if aging effects, such as continued hydration and pore refinement, are not considered. Conversely, using field data with generic aging factors for SCM concretes can lead to underestimations, as these factors depend on a combination of chloride binding and the prolonged hydration processes unique to SCMs. This suggests the need for refined modeling approaches to better represent the long-term chloride transport behavior in SCM concretes, particularly considering the evolving pore structure and binding capacity over time.

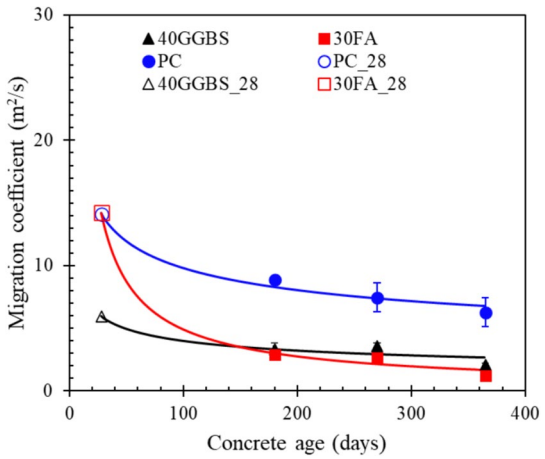

Fig. 3 Plots of migration coefficients as a function of concrete age

As described before, the migration coefficient is a critical parameter for evaluating the transport characteristics of concrete and is often used as a performance indicator for durability (Kara De Maeijer et al., 2020). However, as demonstrated in the results for concrete containing SCMs, relying on migration coefficients measured at an early age (typically 28 days) can lead to ambiguous conclusions regarding long-term durability. To address this limitation, an aging factor should be determined to effectively utilize the migration coefficient as a reliable performance metric. The relationship between migration coefficients and time is modeled by the following equation, as shown in Fig. 3, with the corresponding coefficients provided in Table 4:

$$D_{nssm}(t) = D_{nssm,ref} \left(\frac{t_{ref}}{t} \right)^n (\mathrm{m^2/s}) \quad (4)$$

where $D_{nssm}(t)$ is the predicted migration coefficient at age t (days), $D_{\mathrm{nssm,ref}}$ is the migration coefficient at the reference age (t_{ref} = 28 days), and the exponent n is a constant that indicates the rate of reduction in the migration coefficient over time.

Migration coefficients at 28 days for each mixture were estimated from the literature (Breugel & Polder, 2009;

Table 4 Coefficients for best-fit curves derived from Eq. (4) in Fig. 3

Label	PC	40GGBS	30FA
$D_{\mathrm{nssm,ref}}(\mathrm{m^2/s})$	14.13	5.95	14.23
n	0.29	0.31	0.83
R^2	0.98	0.98	0.99

Park et al., 2016). For example, the coefficient for 30FA concrete was higher than those of other mixtures at 28 days due to the slower hydration associated with FA. The aging factors, derived from the model, were calculated as 0.29 for PC, 0.31 for GGBS, and 0.83 for FA concretes. A higher aging factor corresponds to a more rapid reduction in the migration coefficient over time, reflecting the progressive refinement of the pore structure and continued hydration in SCM concretes. These findings demonstrate that aging factors effectively capture the long-term performance benefits of concrete containing SCMs, highlighting their ability to improve resistance to chloride ingress through sustained hydration processes.

3.3 Electrical Resistivity

The electrical resistivities of the samples used for the compressive strength tests are shown in Fig. 4. As expected, the resistivity of PC concrete was generally lower than that of SCM concretes, except for 30FA samples at 28 days. At this early age, the electrical resistivity of PC concrete was 75.78 Ω·m, compared to 62.91 Ω·m for 30FA concrete. However, after approximately 39 days, the resistivity of 30FA concrete surpassed that of PC concrete. This change can be attributed to the refinement of the pore structure and the reduction in leaching ions, such as Ca^{2+} and OH^-, resulting from pozzolanic reactions during this period, which compensates for the initially higher ionic concentration in the pore solution (Wang & Aslani, 2020). It should be noted that differences in the chemical composition of binders and the dissolution behavior of ions in concrete can lead to significant variations in the ionic concentration of the pore solution. In addition, the rate of pozzolanic reactions and the amount of hydration products formed differ depending on the binder type, resulting in variations in the degree of pore structure refinement. Consequently, these factors simultaneously influence the resistivity of the concrete. This underscores the importance of considering both pore structure refinement and ion content in the pore solution when interpreting resistivity data as a performance indicator.

The resistivity of the pore solution was observed to stabilize after 28 days in the NIST model, as illustrated in Fig. 5. The resistivity of the pore solution was estimated using another model (http://ciks.cbt.nist.gov/poresolncalc.html) (Bentz, 2007). The input data for this model included the degree of hydration and the mixture proportions. The chemical compositions and mixture proportions used in this study are provided in Tables 1 and 2, respectively.

The degree of hydration at 28 days was estimated using a power law model based on the effective water-to-binder ratio (w/b) (L. Tang, 1996). For calculating the equivalent w/b, efficiency factors of 0.6 and 0.4 were applied for 40GGBS and 30FA, respectively, as per BS EN 206 ("BS EN 206 Concrete-Specification, performance, production, and conformity" 2014). Notably, the impact of hydration on pore solution resistivity was relatively negligible after 28 days (Bu & Weiss, 2014).

As shown in Fig. 4, the rate of increase in electrical resistivity slows for PC and 40GGBS concretes during the testing period, while 30FA concrete exhibits a continuous increase in resistivity. At 365 days, in the classification of concrete by corrosion risk in marine environments, 40GGBS and 30FA concretes fall within the moderate corrosion resistance range, whereas PC concrete is classified as having very low resistance (Table 5).

It is important to note that the values used in this classification were obtained from field tests, where the concrete samples were primarily unsaturated. Since electrical

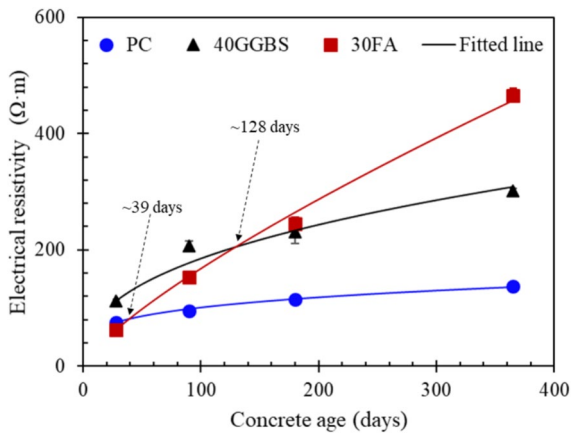

Fig. 4 Electrical resistivity responses of concrete types used in the compressive strength tests

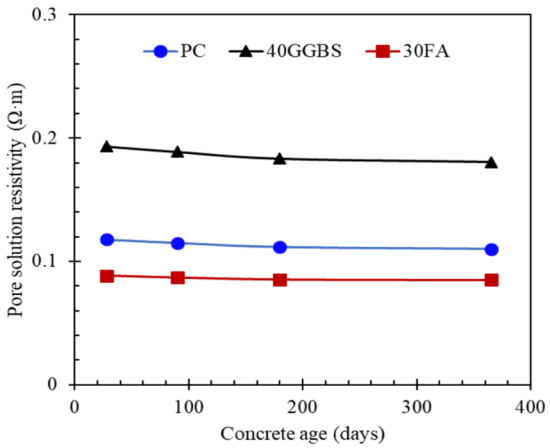

Fig. 5 Pore solution resistivity variations as a function of concrete age (Bentz, 2007)

Table 5 Corrosion resistance clarification with concrete resistivity values for marine concrete (Balestra et al., 2019)

Corrosion resistance	Resistivity (Ωm)
Very low	< 150
Low	150–200
Moderate	200–550
High	550–800
Very high	> 800

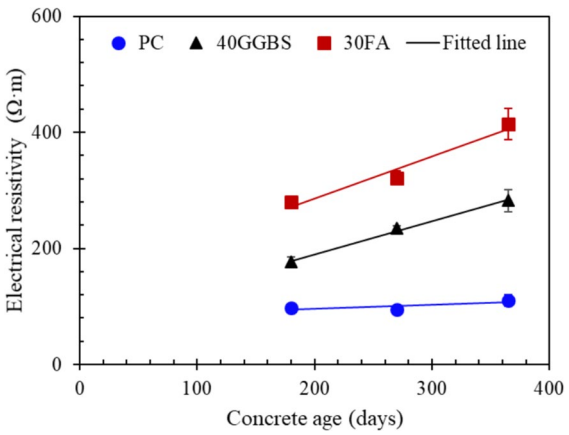

Fig. 6 Electrical resistivity of concrete used in the NT Build 492 test

resistivity is highly sensitive to the moisture content in concrete, this factor must be carefully accounted for to minimize errors in performance evaluation. Moisture content variations can significantly influence resistivity measurements, underscoring the need for controlled testing conditions when assessing the durability of concrete in marine or similar environments. However, compared to other traditional tests such as RCPT or compressive strength, electrical resistivity offers significant advantages, including measurement time, repeatability, and non-destructive measurement. Notably, the long-term resistivity trends in SCM concretes (30FA, 40GGBS) demonstrated sustained increases beyond 28 days due to continued hydration and pore refinement, unlike PC concrete which plateaued. For instance, 30FA concrete exhibited lower resistivity than PC at 28 days but surpassed PC values after 39 days, maintaining an upward trajectory through 365 days. These findings confirm that SCMs significantly enhance long-term durability, as reflected in higher resistivity and improved corrosion resistance.

Figure 6 illustrates the electrical resistivity of concrete samples tested using the NT Build 492 method, along with a linear regression fit (NT Build 492, 1999). The resistivity trends closely mirror those observed in the compressive strength tests. Significant increases in resistivity were observed for 40GGBS and 30FA concretes over the testing period, whereas PC concrete showed only marginal increases. Among the samples, 30FA concrete exhibited the highest resistivity, followed by 40GGBS concrete. It is noteworthy that the vacuum saturation procedure with a saturated $Ca(OH)_2$ solution, as employed in the NT Build 492 test, influences the electrical resistivity results.

To examine the effect of the saturation process on resistivity, comparisons were made between the resistivity of samples saturated with a $Ca(OH)_2$ solution and those tested prior to saturation at 365 days. The scatter plot in Fig. 7 shows the relationship between these conditions, along with an equality line. The data reveal that samples saturated with the $Ca(OH)_2$ solution exhibited lower resistivity than unsaturated samples. This reduction, ranging from 10.0% to 22.8%, is attributed to the enhanced conductivity of the solution filling the micropores under high pressure during saturation (McCarter et al., 2015). These reductions are slightly higher than those reported in previous studies (Spiesz & Brouwers, 2012). The results suggest that concrete with higher inherent resistivity experiences a greater reduction in resistivity due to the saturation process. This behavior can be attributed to the saturation of connected micropores, which are partially or fully unsaturated under normal conditions, with the conductive solution. Thus, the electrical resistivity of concrete is more closely related to chloride transport properties (as evidenced by migration test results) than to mechanical performance (compressive strength).

The relationship between electrical resistivity and curing age can be expressed using the following power equation:

$$\rho(t) = \rho_{\text{ref}} \left(\frac{t}{t_{ref}} \right)^{m} \Omega\text{m} \tag{5}$$

where $\rho(t)$ is the predicted electrical resistivity at age t (d), ρ_{ref} is the electrical resistivity at the reference age t_{ref} (=28 days), and the exponent m is a constant that indicates the increasing rate of the electrical resistivity. The electrical resistivity values at 28 days from the compressive strength tests were used as reference values to predict the resistivity development for migration tests. Best-fitting curves were plotted as regression lines in Figs. 4 and 6. The m values were 0.23, 0.39, and 0.77 for PC, 40GGBS, and 30FA samples, respectively, in the compressive strength tests, and 0.13, 0.33, and 0.74, respectively, in the migration tests. While the estimated values for each mixture are similar due to the same reference

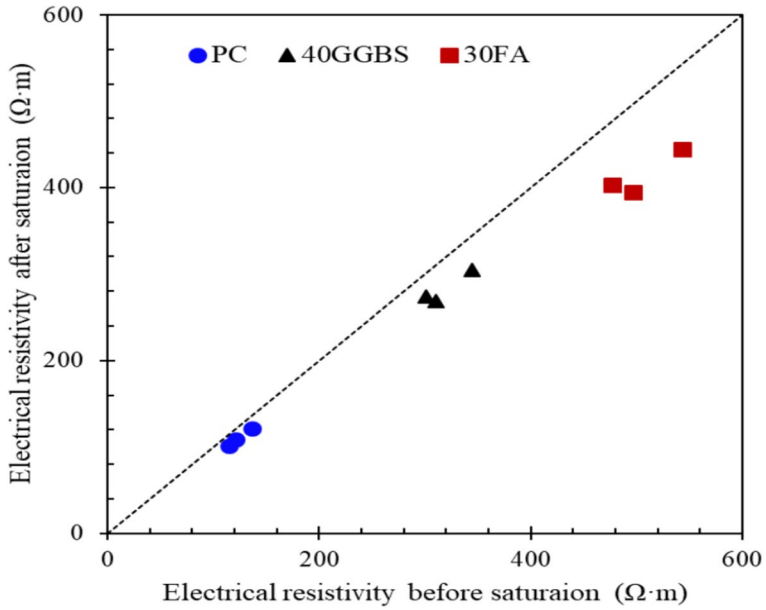

Fig. 7 Comparison of electrical resistivity outcomes of different concrete types before/after saturation

resistivity, the results indicate that the saturation procedure caused lower resistivity values in the migration tests. This highlights the impact of the testing process on electrical resistivity measurements and emphasizes the need for consistency when comparing data across different methods.

4 Discussion

4.1 Determination of Formation Factor

The formation factor, a dimensionless value, was used in this study to evaluate concrete performance and durability over time. This factor in porous materials such as concrete indicates the formation of pore structures by eliminating the effect of the pore solution shown in Eq. 6. The development of the formation factor beyond 365 days was calculated for all mixtures using the following equation:

$$F = \frac{\rho}{\rho_f} \tag{6}$$

where ρ is the measured electrical resistivity, ρ_f is the resistivity of the pore solution, and F is the formation factor at time t (days). Figure 8 illustrates the changes in the formation factor based on the data obtained from the compressive strength tests, as these results were comparable to those from the migration tests. The formation factor increased continuously over time due to the refinement of pores caused by ongoing hydration. Concrete samples containing SCMs exhibited higher formation factors, reflecting the development of tortuous and disconnected pore structures.

The rate of increase in the formation factor for FA concrete remained nearly constant throughout the experimental period, whereas the rate for other mixtures decreased over time. This trend highlights the sustained pozzolanic reaction in FA concrete, which continued to refine the pore structure even at later stages. The results suggest that the refinement of pores, driven by ongoing hydration (pozzolanic reactions and latent hydraulic properties), significantly reduces ionic mobility within the concrete, enhancing resistance to ion ingress (e.g., Cl^-, CO_2, and SO_4^{2-}) in SCM-based concretes. The ranking of the concrete mixtures based on the formation factor at 365 days was as follows: FA40 (5489), GGBS40 (1670), and PC40 (1253). These values indicate that FA concrete provides the highest resistance to ionic transport among the tested mixtures. The formation factor is intrinsically linked to the resistivity of pore water, which is typically estimated using either high-pressure extraction methods or computational models. However, the extraction method is limited to early age concrete (less than 28 days), and modeling requires detailed chemical composition data for the cementitious materials. These limitations underscore the need for further research to enhance the practical applicability of electrical resistivity measurements.

Finally, it is essential to note the critical role of concrete resistivity in controlling corrosion initiation and propagation in reinforced concrete structures. The resistivity influences the movement of ions within the concrete, which governs the corrosion rate of embedded steel after depassivation. A corrosion current is

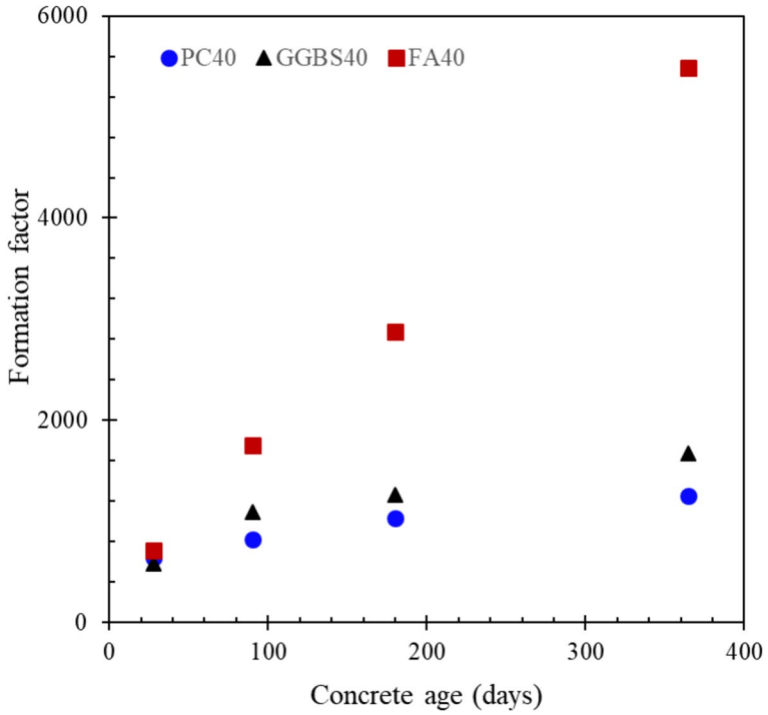

Fig. 8 Scatter plot of formation factors as a function of concrete curing age

generated between the anodic and cathodic areas of the steel in the electrochemical circuit, and higher concrete resistivity effectively reduces this current, thereby lowering the corrosion rate. This makes resistivity a key parameter in designing durable reinforced concrete structures.

4.2 Electrical Resistivity as a Performance/Durability Factor

To establish electrical resistivity as a key indicator of concrete performance and durability, its relationship with performance factors such as compressive strength and migration coefficient was examined. These relationships were analyzed using the equations outlined in earlier sections.

Traditionally, compressive strength has been used to evaluate concrete performance, requiring destructive testing through sample crushing. However, electrical resistivity offers a non-destructive alternative for evaluating or predicting compressive strength (Ferreira & Jalali, 2010; Lübeck et al., 2012). Two types of models, such as empirical and theoretical models, are commonly used to describe the relationship between compressive strength and electrical resistivity. Empirical models rely on regression with time or w/b as independent variables. Theoretical models incorporate nucleation and growth mechanisms of hydration products to predict compressive strength. While these models have been verified for concrete up to 91 days, the evaluation period is often too short to capture the long-term behavior of SCM-based concretes.

The relationship between normalized electrical resistivity and compressive strength is shown in Fig. 9. Electrical resistivity was normalized to the pore solution resistivity at 28 days using the equation:

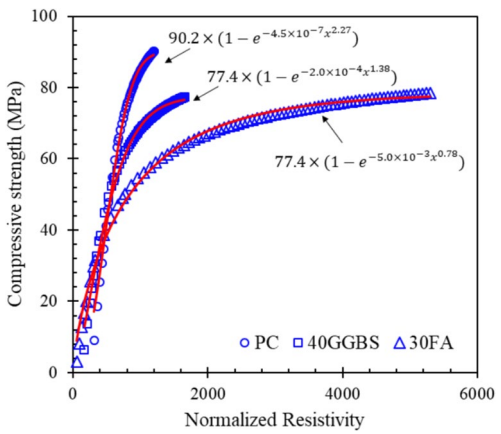

Fig. 9 Plots of compressive strength as a function of normalized resistivity

$$N_\rho = \frac{\rho}{\rho_{f,28}} \tag{7}$$

where ρ is the measured electrical resistivity, $\rho_{f,28}$ is the resistivity of the pore solution at 28 days, and N_ρ is the normalized electrical resistivity. Equation (7) was derived from Eq. (6) based on the observation that pore solution resistivity shows minimal variation after 28 days (as shown in Fig. 5), allowing the changes in normalized electrical resistivity to be primarily attributed to variations in the pore structure of concrete.

As expected, both compressive strength and normalized resistivity increased for all mixtures. A linear relationship was observed up to 500 in normalized resistivity (corresponding to ~ 40 MPa, ~ 55 MPa, and 65 MPa for 30FA, 40GGBS, and PC, respectively). This trend indicates that hydration products related to early age strength development were forming. Beyond this range, the rate of increase slowed, with the 30FA mixture showing continuous improvement due to pore refinement driven by pozzolanic reactions. This relationship can be expressed using a following equation:

$$f(t) = f_{max}\left(1 - e^{-ax^b}\right)(\text{MPa}) \tag{8}$$

where f(x) is the compressive strength, f_{max} is the maximum compressive strength (=365 days in this study),x is the normalized electrical resistivity (N_ρ), and a and b are fitting coefficients.

The transport properties of concrete are critical for assessing its durability. The migration coefficient is a key parameter for quantifying transport behavior and is widely utilized in predictive models, such as Duracrete (Altmann et al., 2012), ClinConc (Tang 2008), and LIFE 365 (M.Ehlen, 2014). However, determining the migration coefficient is labor-intensive and destructive. Electrical resistivity, on the other hand, is directly related to the pore structure of concrete and offers a simpler, faster, and non-destructive alternative. Despite its convenience, quantifying electrical resistivity as a transport property remains challenging. Establishing a clear relationship between electrical resistivity and the migration coefficient is essential to enhance its practical application for concrete durability evaluation.

This study confirmed a strong correlation between electrical resistivity and the migration coefficient. Specifically, low electrical resistivity indicates low resistance to chloride ingress. The relationship between electrical resistivity and the migration coefficient is shown in Fig. 10. To minimize the influence of pore fluid chemistry, all samples in the NT Build 492 test were saturated with a $Ca(OH)_2$ solution, enabling a more reliable assessment of the pore structure's role in electrical resistivity.

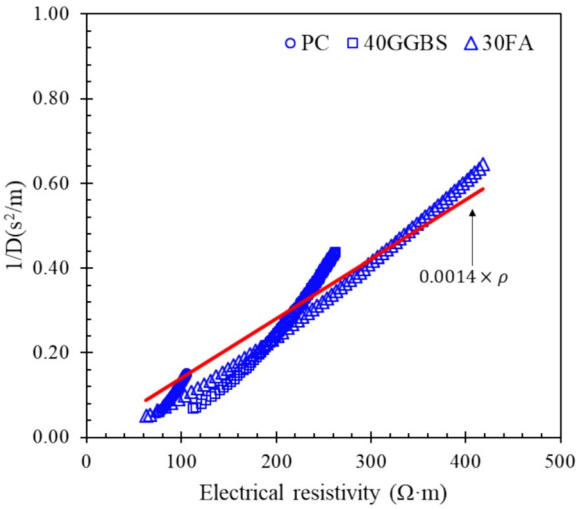

Fig. 10 Plots of migration coefficient as a function of electrical resistivity

According to Kurumisawa and Nawa (Kurumisawa & Nawa, 2016), the Nernst–Planck equation effectively describes the diffusion or migration flux of ions in porous materials, further supporting the theoretical basis for linking electrical resistivity to transport properties:

$$J_i = D_{eff}\frac{\partial C_i}{\partial x} + \frac{z_i F}{RT} D_{eff} C_i \frac{\partial E}{\partial x} \tag{9}$$

where J_i is the flux of the ionic species, D_{eff} is the effective diffusion coefficient, C_i is the concentration of the ionic species, z_i is the valence number of the ionic species, R is the gas constant, F is Faraday's constant, E is the electrical field, and x is the position of the medium. This equation can be simplified using two conditions: (1) no concentration gradient within a pore medium and (2) a large external potential. The flux is then converted into electrical resistivity as follows:

$$\rho = \frac{1}{D_{eff}}\frac{RT}{z_i^2 F^2 C_i} = a \bullet \frac{1}{D_{eff}} \tag{10}$$

where ρ is the bulk electrical resistivity and a is a constant $\left(= \frac{RT}{z_i^2 F^2 C_i}\right)$.

The relationship between electrical resistivity and the migration coefficient can, in theory, be fitted with a single line regardless of the binder type, as described by Eq. 10. However, data scattering was observed in this study, which can be attributed to several factors. First, inconsistencies in reference values played a significant role. Electrical resistivity values were derived from compressive strength tests, while migration coefficients were obtained from the literature at 28 days. Variations in experimental

conditions and sources may have contributed to discrepancies. Second, the gap between theoretical assumptions and experimental results introduced additional variability. Equation 10 assumes a uniform distribution of specific ions within the sample. However, during the NT Build 492 test, the expected "tsunami shape" of the chloride penetration front was not observed. Instead, nonlinear (S-shaped) chloride profiles were recorded, likely due to variations in pore structure and the movement of other ions within the concrete. Finally, measurement limitations contributed to the observed scatter. For migration coefficients, the color-change depths were manually measured after the NT Build 492 test, which introduced potential human error. Similarly, electrical resistivity measurements had an approximate tolerance range of ± 20%, further adding to the variability.

These factors underscore the challenges in establishing a precise and unified relationship between electrical resistivity and migration coefficients. Addressing inconsistencies in reference values, refining measurement techniques, and further investigating ion dynamics and pore structure effects would help bridge the gap between theoretical models and experimental observations, improving the reliability of these correlations.

In this study, regression analyses performed and confirmed strong relationships between resistivity and performance factors. Nonetheless, future work should incorporate confidence intervals and sensitivity analyses to quantify uncertainty and evaluate robustness under varying field conditions. In addition, previous studies have reported that electrical resistance is sensitive to various external environmental influences, such as electrode setup and ambient temperature (Chrisp et al., 2001; McCarter et al., 2005). To reduce errors due to these factors, one should consider applying a temperature correction to the activation energy and obtaining the formation coefficient experimentally or analytically based on the electrode arrangement.

On the other hand, the established correlation between resistivity and migration coefficients enables integration of resistivity measurements into predictive service-life models. For example, field resistivity data can inform inputs for Duracrete, LIFE-365 or ClincConc, allowing performance-based evaluation and maintenance planning. On-site resistivity measurements using handheld probes or embedded sensors could facilitate real-time durability monitoring. Threshold resistivity values could be implemented in specifications to guide acceptance criteria for sustainable concretes.

5 Conclusions

This study investigated the use of electrical resistivity as a performance and durability factor to evaluate compressive strength and transport properties of concretes with different binder types. The results confirmed correlations between electrical resistivity, compressive strength, and migration coefficients. Key findings are summarized below:

- The compressive strengths of PC40, GGBS40, and FA40 concretes were evaluated over time. Concrete containing pozzolanic materials or latent hydraulic binders exhibited slower but continuous strength development. Compressive strengths were modeled as a function of time and binder types, with the parameter values determined as 0.46, 0.50, and 0.65 for PC40, GGBS40, and FA40 concretes, respectively.
- SCM concretes demonstrated lower migration coefficients than PC concrete due to their finer pore structures resulting from continuous hydration. Between 180 and 365 days, the largest reduction (~ 60%) in migration coefficients was observed in FA concrete. Aging factors, which represent the degree of reduction in migration coefficients, were calculated as 0.38, 0.72, and 0.99 for PC, GGBS, and FA concretes, respectively.
- The formation factor, a dimensionless parameter for assessing durability, was evaluated. At 365 days, the formation factors were 1253, 1670, and 5489 for PC, GGBS, and FA concretes, respectively. Higher formation factors indicate better performance and durability. Considering the chemical composition of concrete stabilizes after 28 days, these results underscore the enhanced durability of SCM concretes.
- Electrical resistivity was used to evaluate compressive strengths and migration coefficients, and correlations were confirmed. However, challenges remain due to the influence of various factors on electrical resistivity values. To improve the applicability of this method, further investigations are necessary to quantify the electrical resistivity of the pore solution and reduce the tolerance range of electrical measurements.

In conclusion, while electrical resistivity offers substantial promise for performance-based assessment, limitations remain. It is clear that measurements are sensitive to moisture content, temperature, and pore solution chemistry. Furthermore, electrical resistivity primarily reflects ionic transport and may not capture other deterioration mechanism (e.g., freeze–thaw and carbonation). Thus, resistivity should complement,

not replace, other evaluation methods. Future research should focus on developing standardized correction protocols, refining pore solution modeling, and validating field applications through long-term monitoring.

Acknowledgements
This research presented in this study was supported by the KAIA Research program on the Development of Marine Bridges Operation using Green Energy, funded by the Ministry of Land, Infrastructure and Transport (Grant number: RS-2024-00401101) and by the National Research Foundation of Korea (NRF) grant funded by the Korea government (MSIT) (Grant number: RS-2024-00459490).

Author Contributions
Jaehwan Kim: writing—review and editing, writing—original draft, visualization, validation, methodology, investigation, formal analysis, and conceptualization; Ki-Tae Park: methodology and conceptualization; Jinyoung Yoon: writing—review and editing, writing—original draft, visualization, supervision, methodology, formal analysis, data curation, and conceptualization.

Funding
Ministry of Land, Infrastructure and Transport, RS-2024-00401101, Jaehwan Kim, National Research Foundation of Korea, RS-2024-00459490, Jinyoung Yoon

Availability of Data and Materials
The data and materials are included in the manuscript.

Declarations

Ethics Approval and Consent to Participate
Not applicable.

Consent for Publication
Not applicable.

Competing Interests
The authors declare that they have no known competing financial interests or personal relationships that could have appeared to influence the work reported in this paper.

Received: 17 December 2024 Accepted: 20 May 2025
Published online: 11 August 2025

References

ACI 318-19, Building Code Requirements for Structural Concrete (ACI 318-19). (2019). American Concrete Institute.
Alaswad, G., William John, W. J., & Suryanto, B. (2020). Moisture movement within concrete exposed to simulated hot arid/semi-arid conditions. *Proceedings of the Institution of Civil Engineers - Construction Materials, 173*(6), 298–312. https://doi.org/10.1680/JCOMA.18.00012
Alexander, M. G., Ballim, Y., & Stanish, K. (2008). A framework for use of durability indexes in performance-based design and specifications for reinforced concrete structures. *Materials and Structures, 41*(5), 921–936. https://doi.org/10.1617/S11527-007-9295-0/TABLES/10
Altmann, F., Sickert, J. U., Mechtcherine, V., & Kaliske, M. (2012). A fuzzy-probabilistic durability concept for strain-hardening cement-based composites (SHCCs) exposed to chlorides: Part 1: Concept development. *Cement and Concrete Composites, 34*(6), 754–762. https://doi.org/10.1016/J.CEMCONCOMP.2012.02.014
ASTM C1202-19, Standard Test Method for Electrical Indication of Concrete's Ability to Resist Chloride Ion Penetration. (2019)
Balestra, C. E. T., Nakano, A. Y., Savaris, G., & Medeiros-Junior, R. A. (2019). Reinforcement corrosion risk of marine concrete structures evaluated through electrical resistivity: Proposal of parameters based on field structures. *Ocean Engineering, 187*, 106167.
Bentz, D. P. (2007). A virtual rapid chloride permeability test. *Cement and Concrete Composites, 29*(10), 723–731. https://doi.org/10.1016/J.CEMCONCOMP.2007.06.006
Breugel, K. van, & Polder, R. (2009). Probability-based service life design of structural concrete. In 2nd Int RILEM Workshop on Concrete Durability- and Service Life Planning-ConcreteLife'09 (pp. 383–391)
BS EN 1992-1-1:2004+A1:2014 Eurocode 2: Design of concrete structures - Part 1–1: General rules and rules for buildings. (2014).
BS EN 206 Concrete-Specification, performance, production, and conformity. (2014).
Bu, Y., & Weiss, J. (2014). The influence of alkali content on the electrical resistivity and transport properties of cementitious materials. *Cement and Concrete Composites, 51*, 49–58. https://doi.org/10.1016/J.CEMCONCOMP.2014.02.008
Cai, R., Tian, Z., Ye, H., He, Z., & Tang, S. (2021). The role of metakaolin in pore structure evolution of Portland cement pastes revealed by an impedance approach. *Cement and Concrete Composites, 119*, 103999. https://doi.org/10.1016/J.CEMCONCOMP.2021.103999
Chidiac, S. E., & Shafikhani, M. (2020). Electrical resistivity model for quantifying concrete chloride diffusion coefficient. *Cement and Concrete Composites, 113*, 103707. https://doi.org/10.1016/J.CEMCONCOMP.2020.103707
Chrisp, T. M., Starrs, G., McCarter, W. J., Rouchotas, E., & Blewett, J. (2001). Temperature-conductivity relationships for concrete: An activation energy approach. *Journal of Materials Science Letters, 20*, 1085–1087. https://doi.org/10.1023/A:1010926426753
Ferreira, R. M., & Jalali, S. (2010). NDT measurements for the prediction of 28-day compressive strength. *NDT & E International, 43*(2), 55–61. https://doi.org/10.1016/J.NDTEINT.2009.09.003
Hinrichs, W., & Odler, I. (2015). Investigation of the hydration of Portland blast-furnace slag cement: Hydration kinetics. *Advances in Cement Research, 2*(5), 9–13. https://doi.org/10.1680/ADCR.1989.2.5.9
Huang, L., Tang, L., Löfgren, I., Olsson, N., Yang, Z., & Li, Y. (2022). Moisture and ion transport properties in blended pastes and their relation to the refined pore structure. *Cement and Concrete Research, 161*, 106949. https://doi.org/10.1016/J.CEMCONRES.2022.106949
Kara De Maeijer, P., Craeye, B., Snellings, R., Kazemi-Kamyab, H., Loots, M., Janssens, K., & Nuyts, G. (2020). Effect of ultra-fine fly ash on concrete performance and durability. *Construction and Building Materials, 263*, 120493. https://doi.org/10.1016/J.CONBUILDMAT.2020.120493
Kessy, J. G., Alexander, M. G., & Beushausen, H. (2015). Concrete durability standards: International trends and the South African context. *Journal of the South African Institution of Civil Engineering, 57*(1), 47–58. https://doi.org/10.17159/2309-8775/2015/V57N1A5
Kim, J., Suryanto, B., & McCarter, W. J. (2019). Conduction, relaxation and complex impedance studies on Portland cement mortars during freezing and thawing. *Cold Regions Science and Technology, 166*, 102819. https://doi.org/10.1016/J.COLDREGIONS.2019.102819
KS F 2405:2010 Standard test method for compressive strength of concrete. (2010).
KS F 2560:2019 Chemical admixtures for concrete. (2019).
KS L 5201:2016 Portland cement. (2016).
KS L 5210:2017 Portland blast-furnace slag cement. (2017).
KS L 5405:2018 Fly ash. (2018).
Kurumisawa, K., & Nawa, T. (2016). Electrical conductivity and chloride ingress in hardened cement paste. *Journal of Advanced Concrete Technology, 14*(3), 87–94. https://doi.org/10.3151/JACT.14.87
Lübeck, A., Gastaldini, A. L. G., Barin, D. S., & Siqueira, H. C. (2012). Compressive strength and electrical properties of concrete with white Portland cement and blast-furnace slag. *Cement and Concrete Composites, 34*(3), 392–399. https://doi.org/10.1016/J.CEMCONCOMP.2011.11.017
M.Ehlen. (2014). LIFE-365 Service Life Prediction Model, Version 2.2.1—User's Manual.
McCarter, W. J., Chrisp, T. M., Starrs, G., Basheer, P. A. M., & Blewett, J. (2005). Field monitoring of electrical conductivity of cover-zone concrete. *Cement and Concrete Composites, 27*(7–8), 809–817. https://doi.org/10.1016/J.CEMCONCOMP.2005.03.008
McCarter, W., Suryanto, B., Abdalgadir, H. T., Starrs, G., & Kim, J. (2022). Features of immittance spectra as performance indicators for cement-based concretes. *Advances in Cement Research, 35*(10), 452–465. https://doi.org/10.1680/JADCR.22.00023/ASSET/IMAGES/SMALL/JADCR.22.00023-F7.GIF

McCarter, W. J., Taha, H. M., Suryanto, B., & Starrs, G. (2015). Two-point concrete resistivity measurements: Interfacial phenomena at the electrode–concrete contact zone. *Measurement Science and Technology, 26*(8), 085007. https://doi.org/10.1088/0957-0233/26/8/085007

Newlands, M. D., Jones, M. R., Kandasami, S., & Harrison, T. A. (2008). Sensitivity of electrode contact solutions and contact pressure in assessing electrical resistivity of concrete. *Materials and Structures, 41*(4), 621–632. https://doi.org/10.1617/S11527-007-9257-6/FIGURES/10

NT Build 492 (1999). Concrete, mortar and cement-based repair materials: Chloride migration coefficient from non-steady-state migration experiments.

Park, J.-I., Lee, K.-M., Kwon, S.-O., Bae, S.-H., Jung, S.-H., & Yoo, S.-W. (2016). Diffusion decay coefficient for chloride ions of concrete containing mineral admixtures. *Advances in Materials Science and Engineering*. https://doi.org/10.1155/2016/2042918

PD CEN/TR 16563:2013 Principles of the equivalent durability procedure. (2013).

Polder, R. B. (2001). Test methods for on site measurement of resistivity of concrete—a RILEM TC-154 technical recommendation. *Construction and Building Materials, 15*(2–3), 125–131. https://doi.org/10.1016/S0950-0618(00)00061-1

Sangoju, B., Gopal, R., Bhajantri, H., & B. (2021). A review on performance-based specifications toward concrete durability. *Structural Concrete, 22*(5), 2526–2538. https://doi.org/10.1002/SUCO.201900542

Spiesz, P., & Brouwers, H. J. H. (2012). Influence of the applied voltage on the Rapid Chloride Migration (RCM) test. *Cement and Concrete Research, 42*(8), 1072–1082. https://doi.org/10.1016/J.CEMCONRES.2012.04.007

Standard Specifications for Concrete Structures: Materials and Construction. (2007).

Sun, J., Jin, Z., Chang, H., & Zhang, W. (2024). A review of chloride transport in concrete exposed to the marine atmosphere zone environment: Experiments and numerical models. *Journal of Building Engineering, 84*, 108591. https://doi.org/10.1016/J.JOBE.2024.108591

Tang, L. (1996). *Chloride transport in concrete-measurement and prediction*. Chalmers University of Technology.

Tang, L. (2008). Engineering expression of the ClinConc model for prediction of free and total chloride ingress in submerged marine concrete. *Cement and Concrete Research, 38*(8–9), 1092–1097. https://doi.org/10.1016/J.CEMCONRES.2008.03.008

Tang, L., Nilsson, L.-O., & Basheer, P. A. M. (2012). *Resistance of concrete to chloride ingress: testing and modelling*. Taylor & Francis Group.

Tibbetts, C. M., Paris, J. M., Ferraro, C. C., Riding, K. A., & Townsend, T. G. (2020). Relating water permeability to electrical resistivity and chloride penetrability of concrete containing different supplementary cementitious materials. *Cement and Concrete Composites, 107*, 103491. https://doi.org/10.1016/J.CEMCONCOMP.2019.103491

Tong, L. Y., Xiong, Q. X., Zhang, M., Meng, Z., Meftah, F., & Liu, Q. F. (2023). Multi-scale modelling and statistical analysis of heterogeneous characteristics effect on chloride transport properties in concrete. *Construction and Building Materials, 367*, 130096. https://doi.org/10.1016/J.CONBUILDMAT.2022.130096

Tuutti, K. (1982). *Corrosion of Steel in Concrete*. Lund University.

Wang, L., & Aslani, F. (2020). Electrical resistivity and piezoresistivity of cement mortar containing ground granulated blast furnace slag. *Construction and Building Materials, 263*, 120243. https://doi.org/10.1016/J.CONBUILDMAT.2020.120243

Yamamoto, M., Nakarai, K., Yoshizumi, Y., & Torrent, R. (2024). Relationship between chloride ingress and concrete cover quality of inland structures exposed to deicing salts. *Case Studies in Construction Materials, 20*, Article e03075. https://doi.org/10.1016/J.CSCM.2024.E03075

Yuan, Q., Shi, C., De Schutter, G., Audenaert, K., & Deng, D. (2009). Chloride binding of cement-based materials subjected to external chloride environment—A review. *Construction and Building Materials, 23*(1), 1–13. https://doi.org/10.1016/J.CONBUILDMAT.2008.02.004

Zhang, M., Sun, S., Liu, K., Li, T., & Yang, H. (2023). Research on the critical chloride content of reinforcement corrosion in marine concrete—A review. *Journal of Building Engineering, 79*, 107838. https://doi.org/10.1016/J.JOBE.2023.107838

Publisher's Note

Jaehwan Kim Senior researcher at Korea Institute of Civil Engineering and Building Technology. His major research interest includes evaluating concrete performance using electrical measurement.

Ki-Tae Park Senior research fellow at Korea Institute of Civil Engineering and Building Technology. His major research interest includes Development of bridge maintenance technology.

Jinyoung Yoon Assistant Professor at Konkuk University (Department of Civil and Environmental Engineering). His major research interest includes development of advanced and sustainable construction materials.